ORGANOMETALLICS

pubs.acs.org/Organometallics Article

Divergent Solution and Solid-State Structures of Mono- and Dinuclear Nickel(II) Pyridone Complexes

Sean T. Goralski, Taylor A. Manes, Simone E. A. Lumsden, Vincent M. Lynch, and Michael J. Rose*

Cite This: https://dx.doi.org/10.1021/acs.organomet.9b00799 Read Online

ACCESS | Metrics & More | Article Recommendations | Supporting Information

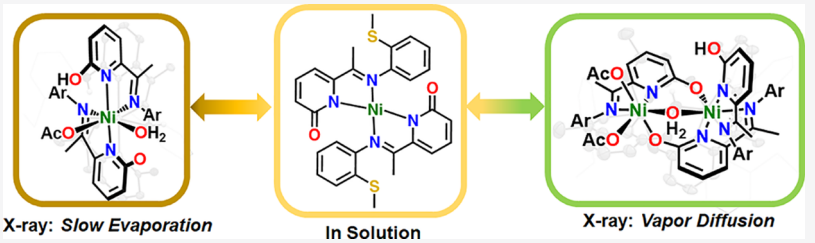

ABSTRACT: The chelating 2-pyridone ligand (*E*)-6-(1-((2-(methylthio)phenyl)imino)ethyl)pyridin-2(1*H*)-one (**1**) has been used to synthesize five nickel(II) complexes that have been characterized by single-crystal X-ray diffraction, UV/vis and IR spectroscopies, and benchtop magnetometry. Reaction of NiX_2 (X = BF_4, Cl) with **1** yielded the C_2-symmetric halide-bridged Ni dimers $[(\mu\text{-}F)Ni_2(\kappa N,N,O\text{-}\mathbf{1}^-)_2(\kappa N,N\text{-}\mathbf{1})_2](BF_4)$ (**2**) and $[(\mu\text{-}Cl)Ni_2(\kappa N,N,O\text{-}\mathbf{1}^-)_2(\kappa N,N\text{-}\mathbf{1}^-)(\kappa N,N\text{-}\mathbf{1})]$ (**3**), where **2** is formed via a rare example of fluoride abstraction from BF_4^- by a transition metal. Remarkably, the reaction of $Ni(OAc)_2$ with **1** followed by different methods of crystallization yielded three different products: the *dimer* $[(\mu\text{-}OH_2)Ni_2(\kappa N,N,O\text{-}\mathbf{1}^-)(\kappa N,N\text{-}\mathbf{1}^-)(\kappa N,N\text{-}\mathbf{1})(OAc)_2]$ (**4**), as well as the *monomers* $[Ni(\kappa N,N\text{-}\mathbf{1}^-)_2(MeOH)_2]$ (**5**) and $[Ni(\kappa N,N\text{-}\mathbf{1}^-)(\kappa N,N\text{-}\mathbf{1})(OAc)(OH_2)]$ (**6**). This observation is emblematic of the soft energy landscape of coordination motifs and nuclearity that pyridone ligands provide with late 3d transition metals. To better understand the solution versus solid-state speciation, solid-state UV/vis reflectance and solution-state UV/vis absorbance spectra were obtained. Surprisingly, the solution-state UV/vis spectra of **4** and **6** each provided nearly identical absorption spectra ($\lambda_{max} \approx 360$ nm), which matched neither of the solid-state reflectance spectra of **4** or **6** ($\lambda \approx 590$, 790, 970 nm; $^3A_{2g} \rightarrow {}^3T_{1g}$, $^3A_{2g} \rightarrow {}^1E_{2g}$, and $^3A_{2g} \rightarrow {}^3T_{2g}$, respectively). Rather, the solution spectra are consistent only with the spectroscopic features (MLCT) of a conventional square-planar Ni(II) species.

INTRODUCTION

The N-heterocyclic ligand 2-pyridone displays a rich coordination chemistry with the transition metals. Pyridones found their first major application in the 1980s as 1,3-heteroatomic bridging ligands to enforce M−M multiple bonds,[1−3] and there are now thousands of reported transition-metal−pyridone structures, showcasing the wide variety of binding motifs that 2-pyridone and its derivatives can adopt. While this class of ligands has seen use across a broad range of applications over the last 40 years—ranging from the synthesis of polynuclear metal clusters exhibiting extremely high spin values[4,5] to application in various catalytic transformations such as transfer hydrogenation,[6−9] alcohol dehydrogenation,[10,11,19,38] and water oxidation[12−14]—the fundamental factors that underpin the coordination motifs of 2-pyridone ligands remains fairly unexplored. A 2-pyridone can adopt any of eight ligation motifs, complexing one, two, or three metal centers (Figure 1). This diversity in binding modes is especially notable for the first-row late transition metals (Mn, Fe, Co, Ni, Cu, Zn).

Nickel(II), in particular, exhibits great structural diversity in its coordination chemistry with 2-pyridones (Figure 2 for examples). The majority of reported Ni−pyridone structures exhibit high nuclearity, containing 6−12 nickel centers. For example, Winpenny and co-workers leveraged the propensity for

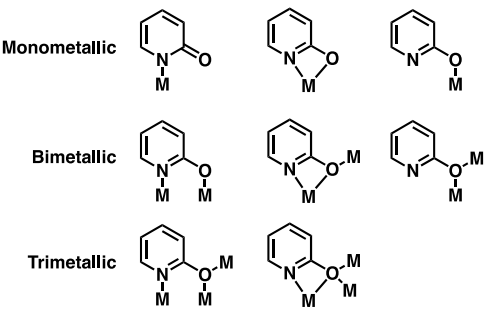

Figure 1. Possible binding modes adopted by a 2-pyridone ligand in the presence of transition metal(s).

Special Issue: Organometallic Chemistry at Various Length Scales

Received: November 25, 2019

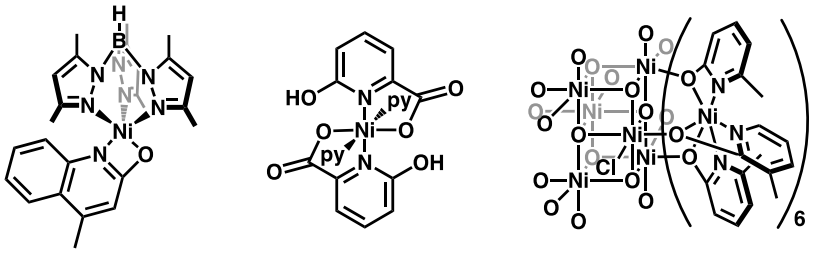

Figure 2. Examples of previously characterized Ni−pyridone metal complexes.

nickel to form polynuclear oxo-bridged clusters in the presence of 2-pyridone ligands to synthesize so-called "metal cages" to study the relationship between the structure and magnetic properties of metal and metal oxide materials,[15,18] with application in data storage using single-molecule magnets.[4,16,17] While great focus has been given to Ni−pyridone complexes of high nuclearity, comparatively less attention has been paid to the synthetic control of mononuclear Ni−pyridone complexes. Seven monomeric Ni−pyridone complexes have been reported in the literature (excluding families of closely related compounds), and it is notable that all of these structures contain either polydentate supporting ligands—such as scorpionate[19] or triazacyclododecane[20]—or a pyridone ligand that is, itself, polydentate.[21−23] These polydentate ligands block coordination sites at the nickel center, thus hindering pyridone ligands from achieving high nuclearity. It has also been observed that the formation of lower-nuclearity Ni−pyridone complexes is favored when the reaction and crystallization are performed in polar solvents such as methanol, ethanol, and acetonitrile.[24]

With these observations in mind, this work strives to determine a set of experimental conditions in which nickel−pyridone complexes of low nuclearity can be obtained. We use a tridentate *NNS*-pyridone ligand (Scheme 1) in accordance with

Scheme 1. Synthesis of NNS Pyridone Ligand 1[a]

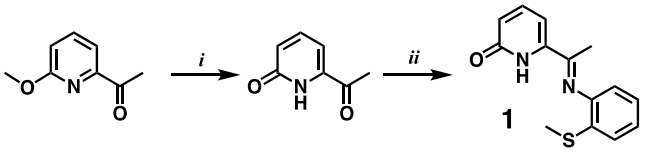

[a]Legend: (i) HCl, dioxane, 80 °C, 20 h (61%); (ii) 2-(methylthio)-aniline, TsOH, ^{n}BuOH, reflux, 18 h (34%).

the observation that polydentate ligands hinder bridging. The ligand was complexed with Ni(II) salts under varying solvent and counterion conditions. From this study, five Ni−pyridone complexes have been isolated and characterized: two mononuclear and three dinuclear complexes. This is the first report of homometallic dinuclear pyridone-bridged nickel complexes. For one of these complexes, we discovered a rare example of transition-metal-mediated fluoride abstraction from tetrafluoroborate, yielding a fluoride-bridged nickel dimer. Additionally, UV/vis spectroscopy revealed that complexes **4** and **6** do not retain their crystallographically determined structures in solution but rather exist in solution as diamagnetic square-planar complexes. This report of coordinatively flexible pyridone−transition metal complexes expands on a scant collection of observations and comments throughout the inorganic and organometallic literature regarding the diverse and unpredictable ligation of 2-pyridone derivatives. For example, proposed mechanisms for hydrogenation/dehydrogenation reactions catalyzed by nickel(II) pyridones often invoke a switching between κN and κN,O ligation of the pyridone ligand though the catalytic cycle.[19,38] Additionally, Papish and co-workers noted that reacting 6,6′-dihydroxybipyridine with copper(II) sulfate results in a monometallic complex, while the reaction of the same ligand with copper(II) nitrate results in a bi- or trimetallic copper complex (depending on pH).[37] In this work, we importantly note that this structural diversity in the solid state diverges from a single solution-state species.

EXPERIMENTAL SECTION

General Procedures and Reagents. All commercially available reagents were used without further purification. The reagents 2-acetyl-6-methoxypyridine (Alfa Aesar), *p*-toluenesulfonic acid monohydrate (Chem Impex, Intl.), sodium hydride (Sigma-Aldrich), nickel(II) acetate tetrahydrate (Acros Organics), nickel(II) chloride hexahydrate (Sigma-Aldrich), and nickel(II) tetrafluoroborate hexahydrate (Alfa Aesar) were all purchased and used without further purification. The 2-(methylthio)aniline (Oakwood Chemical) was freshly distilled before use. Deuterochloroform was purchased from Cambridge Isotope Laboratories and used without further purification.

Physical Measurements. All NMR spectra were acquired on a Varian DirectDrive spectrometer (400 MHz), and the reported chemical shifts are referenced to chloroform. Mass spectrometry (MS) data were collected on an Agilent Technologies 6530 Accurate Mass Q-TOF LC/MS (ESI) or Micromass Autospec Ultima (CI). Magnetic susceptibility measurements were performed on an Alfa Aesar MSB-1 magnetic susceptibility balance, wherein samples were ground into a fine powder and packed into 4 mm diameter quartz tubes. IR spectra were collected on a Bruker Alpha Fourier transform infrared (FTIR) spectrometer equipped with a diamond ATR crystal; all samples were analyzed as solids. UV/vis absorption and reflectance spectra were acquired using a Shimadzu UV-2600 UV/vis spectrophotometer. Solution samples (absorbance) were prepared as ∼0.2 mg/mL solutions in DCM in a fused quartz cuvette, and solid samples (reflectance) were prepared by applying finely powderized crystals of each compound to a fused quartz slide.

Ligand Synthesis. *2-Acetylpyridin-2(1H)-one.* Commercially available 2-acetyl-6-methoxypyridine (2.00 g, 12.3 mmol) was dissolved in 40 mL of dioxane. To this was added 4 M hydrochloric acid (20 mL, 80 mmol). The reaction mixture was heated to 80 °C for 20 h. The yellow solution was concentrated under vacuum until white crystals began to precipitate. The mixture was cooled to 0 °C in an ice/water bath to further precipitate the product. The solid was collected by vacuum filtration and washed with a small amount of cold acetone to afford a white crystalline product. Yield: 1.408 g (61.2%) ^{1}H NMR (400 MHz, $CDCl_3$), δ in ppm: 9.64 (s, 1H), 7.48 (dd, 1H), 6.88 (dd, 1H), 6.83 (dd, 1H), 2.54 (s, 3H). ^{13}C NMR (400 MHz, $CDCl_3$), δ in ppm: 190.58, 167.98, 161.82, 139.64, 138.79, 128.16, 109.87, 24.70. FTIR (selected peaks): ν 1685, 1645 cm^{-1} (C═O stretches). HRMS (CI+) *m*/*z*: $[M]^+$ calcd for $C_7H_7NO_2$ 137.0477; found 137.0474.

https://dx.doi.org/10.1021/acs.organomet.9b00799
Organometallics XXXX, XXX, XXX−XXX

Scheme 2. Metalation of 1 with Various Ni(II) Sources and Solid-State Products as Determined by the Indicated Modes of Crystallization

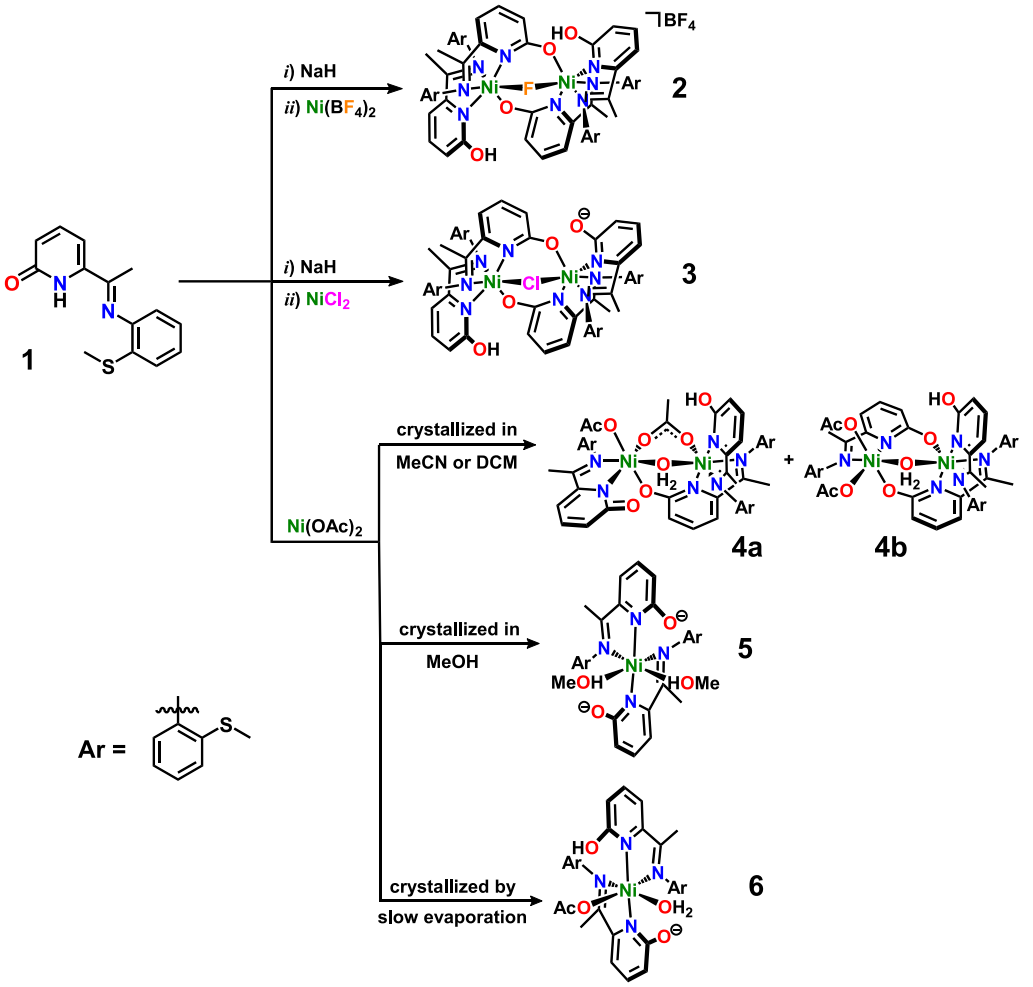

*(E)-6-(1-((2-(Methylthio)phenyl)imino)ethyl)pyridin-2(1H)-one (**1**).* The product from the above reaction (2-acetyl-6-hydroxypyridin-1-ium hydrochloride; 1.41 g, 8.12 mmol) was dissolved in 300 mL of *n*-butanol. To this was added 2-(methylthio)aniline (1.70 g, 12.18 mmol) followed by *p*-toluenesulfonic acid (0.23 g, 1.22 mmol). The reaction flask was fitted with a Dean−Stark trap, and the mixture was refluxed under nitrogen for 18 h. The solvent was removed under vacuum to yield a brown oil. This crude product was purified by a silica gel column (first 10:1 DCM/acetone and then 5:1 DCM/acetone) to afford a yellow solid. Yield: 0.71 g (34%) ^{1}H NMR (400 MHz, $CDCl_3$), δ in ppm: 10.30 (s, 1H), 7.46 (dd, 1H), 7.25 (dd, 1H), 7.16 (m, 2H), 6.73 (d, 1H), 6.66 (d, 1H), 6.64 (dd, 1 H) 2.40 (s, 3H), 2.14 (s, 3H). ^{13}C NMR (400 MHz, $CDCl_3$), δ in ppm: 162.33, 158.62, 146.08, 141.20, 139.97, 129.89, 125.73, 125.49, 125.30, 125.28, 118.67, 107.30, 15.59, 15.12. FTIR (selected peaks): ν 1651 cm^{-1} (C═O stretch). HRMS (+ESI) *m*/*z*: $[M + H]^+$ calcd for $C_{14}H_{14}N_2OS$ 259.0900; found 259.0898.

Syntheses of Metal Complexes. *[(μ-F)Ni$_2$(κN,N,O-**1**$^-$)$_2$(κN,N-**1**)$_2$](BF$_4$) (**2**).* Ligand **1** (50.0 mg, 0.194 mmol) was dissolved in 3 mL of *N*,*N*-dimethylformamide (DMF), methanol (MeOH) or acetonitrile (MeCN) as a yellow solution. To this solution was added NaH (5.0 mg, 0.208 mmol); upon addition, hydrogen gas was evolved. With stirring, $[Ni(H_2O)_6](BF_4)_2$ (62.7 mg, 0.178 mmol) was added in one portion. The solution was stirred for 30 min at room temperature, and it slowly turned green. The solvent was removed under vacuum to afford a green solid. This was dissolved in a minimal amount of DMF, MeOH, MeCN, or dichloromethane (DCM). Slow vapor diffusion of diethyl ether (Et_2O) into this solution (any solvent) at room temperature provided green crystals of **2** suitable for X-ray diffraction. Yield (X-ray-quality crystals): 10% (26 mg). FTIR (selected peaks): ν 1624, 1611, 1600, 1579 cm^{-1} (C═O and C═N stretches). Magnetic susceptibility (298 K): μ_{eff} = 4.12 μ_B. Anal. Calcd for $C_{56}H_{56}F_5N_8Ni_2O_5S_4$: C, 52.69; H, 4.74; N, 8.78. Found: C, 49.88; H, 3.99; N, 6.18.

*[(μ-Cl)Ni$_2$(κN,N,O-**1**$^-$)$_2$(κN,N-**1**)(κN,N-**1**)] (**3**).* Ligand **1** (50.0 mg, 0.194 mmol) was dissolved in 3 mL of DMF, MeOH, or MeCN to generate a yellow solution. To this solution was added NaH (5.0 mg, 0.208 mmol); upon addition, hydrogen gas was evolved. With stirring, $[Ni(Cl)_2(H_2O)_4]\cdot 2H_2O$ (43.8 mg, 0.178 mmol) was added in one portion. The solution was stirred for 30 min at room temperature, and the solution slowly turned green. The solvent was removed under vacuum to afford a green solid, which was dissolved in a minimal amount of DMF, MeOH, MeCN, or DCM. Slow vapor diffusion of Et_2O into this solution at room temperature yielded green crystals of **3** suitable for X-ray diffraction. Yield (X-ray-quality crystals): 9.7% (26 mg). FTIR (selected peaks): ν 1617, 1598, 1578 cm^{-1} (C═O and C═N stretches). Magnetic susceptibility (298 K): μ_{eff} = 4.24 μ_B. Anal. Calcd for $C_{60}H_{67}ClN_8Ni_2O_5S_4$: C, 57.14; H, 5.35; N, 8.88. Found: C, 55.98; H, 4.52; N, 7.92.

*[(μ-OH$_2$)Ni$_2$(**1**)$_3$(OAc)$_2$] (**4**).* Ligand **1** (50.0 mg, 0.194 mmol) was dissolved in 3 mL of either MeCN or dichloromethane (DCM) to generate a yellow solution. With stirring, commercially available nickel(II) acetate ($[Ni(OAc)_2(H_2O)_4]$; 32.5 mg, 0.178 mmol) was added in one portion. The solution was stirred for 30 min at room temperature, and it slowly turned dark yellow-brown. The solvent was removed under vacuum to afford a yellow-brown solid, which was dissolved in a minimal amount of either MeCN or DCM. Slow vapor diffusion of Et_2O into this solution at room temperature provided green crystals of **4** suitable for X-ray diffraction. Yield (X-ray-quality crystals):

https://dx.doi.org/10.1021/acs.organomet.9b00799
Organometallics XXXX, XXX, XXX−XXX

9.9% (20 mg). FTIR (selected peaks): ν 1743, 1728, 1616, 1599, 1582 cm^{-1} (C═O and C═N stretches). Magnetic susceptibility (298 K): μ_{eff} = 4.05 μ_B. Anal. Calcd for $C_{46}H_{51}N_6Ni_2O_8S_3$: C, 53.67; H, 4.99; N, 8.16. Found: C, 52.11; H, 4.84; N, 7.92.

*[Ni(κN,N-**1**$^-$)$_2$(MeOH)$_2$] (**5**).* Ligand **1** (50.0 mg, 0.194 mmol) was dissolved in 3 mL of MeOH to generate a yellow solution. With stirring, nickel(II) acetate (32.5 mg, 0.178 mmol) was added in one portion. The solution was stirred for 30 min at room temperature, and it slowly changed to olive green. The solvent was removed under vacuum to afford a green solid, which was dissolved in a minimal amount of methanol. Slow vapor diffusion of Et_2O into this solution at room temperature provided yellow crystals suitable for X-ray diffraction. Yield (X-ray-quality crystals): 21% (28 mg). FTIR (selected peaks): ν 1623, 1600, 1578, 1544 cm^{-1} (C═O and C═N stretches). Magnetic susceptibility (298 K): μ_{eff} = 2.88 μ_B. Anal. Calcd for $C_{32}H_{48}N_4NiO_7S_2$: C, 53.12; H, 6.69; N, 7.74. Found: C, 52.83; H, 6.55; N, 7.50.

*[Ni(κN,N-**1**$^-$)(κN,N-**1**)(OAc)(OH$_2$)] (**6**).* Ligand **1** (50.0 mg, 0.194 mmol) was dissolved in 3 mL of MeCN to generate a yellow solution. With stirring, nickel(II) acetate (32.5 mg, 0.178 mmol) was added in one portion. The solution was stirred for 30 min at room temperature, and it slowly changed to dark yellow-brown. The solvent was removed under vacuum to afford a yellow-brown solid, which was dissolved in a minimal amount of MeCN. Slow evaporation of the solvent at −20 °C provided yellow crystals suitable for X-ray diffraction. Yield (X-ray-quality crystals): 15% (21 mg). FTIR (selected peaks): ν 1739, 1614, 1597, 1580 cm^{-1} (C═O and C═N stretches). Magnetic susceptibility (298 K): μ_{eff} = 2.89 μ_B. Anal. Calcd for $C_{32}H_{40}N_5NiO_6S_2$: C, 53.87; H, 5.65; N, 9.82. Found: C, 51.67; H, 4.47; N, 9.08.

RESULTS AND DISCUSSION

Synthesis of Ligand and Metal Complexes. The pyridone-containing NNS ligand (**1**) used in this study was synthesized in two steps from commercially available starting materials (Scheme 1). The precursor 2-acyl-6-methoxypyridine was first demethylated by heating with hydrochloric acid for 20 h to obtain 2-acetylpyridin-2(1*H*)-one in 61% yield.[25] This synthon was then condensed with 2-(methylthio)aniline to provide the NNS ligand in 34% yield. The broad singlet at δ 10.31 ppm in the ^{1}H NMR spectrum of **1** is indicative of a pyridone N*H* proton, indicating that, in solution, the pyridone tautomer of **1** is dominant, rather than the pyridinol tautomer. This observation was corroborated by FTIR spectroscopy of the solid (ν_{CO} 1653 cm^{-1}) as well as the structure obtained by single-crystal X-ray diffraction (Supporting Information) where a C═O bond distance of 1.246(5) Å was observed (typical C═O bond lengths for pyridones range from 1.23 to 1.27 Å). The design of this ligand was intended to enforce the formation of low-nuclearity Ni−pyridone complexes, while maintaining a relatively simple structure that is synthetically accessible. Relatedly, our group has reported that pyridine analogues of **1** bind Fe(II) through the pyridine nitrogen, imine nitrogen, and thioether sulfur in a pincer fashion.[27]

With **1** in hand, we investigated complexations with various Ni(II) salts in several solvents (Scheme 2). The reaction procedure included *in situ* deprotonation of **1** to generate its anion **1**$^-$ by reaction with either sodium hydride or $Ni(OAc)_2$, followed by addition of $NiX_2{\cdot}nH_2O$ (where X = OAc^-, Cl^-, BF_4^-). These Ni(II) salts were chosen to investigate a range of anions: acetate, which is a strong 1,3-bridging ligand, chloride, which is a less strong μ_2-bridging ligand, and tetrafluoroborate, which is nominally noncoordinating. To investigate the effect of solvent on the nuclearity of the product, the reactions were performed in DMF, MeOH, MeCN, and DCM, spanning a range of solvent polarities and including one polar, protic solvent. For all experiments, the reaction and crystallization were performed in the same solvent.

X-ray Crystal Structures. *[Ni$_2$(**1**)$_4$(F)](BF$_4$) (**2**).* The complex $[(\mu\text{-F})Ni_2(\kappa N,N,O\text{-}\mathbf{1}^-)_2(\kappa N,N\text{-}\mathbf{1})_2](BF_4)$ (**2**) was synthesized by the reaction of **1**$^-$ (generated *in situ* by reaction with sodium hydride) with $[Ni(H_2O)_6)](BF_4)_2$. The resulting green solution was evaporated to afford a light green powder; the choice of solvent for the reaction and crystallization had no effect on the isolated product. Reaction followed by crystallization (slow vapor diffusion of diethyl ether at −20 °C) from DCM, MeCN, MeOH, or DMF all resulted in green blocklike crystals suitable for single-crystal X-ray diffraction. The structure of complex **2** as determined by XRD (Figure 3) is a C_2-

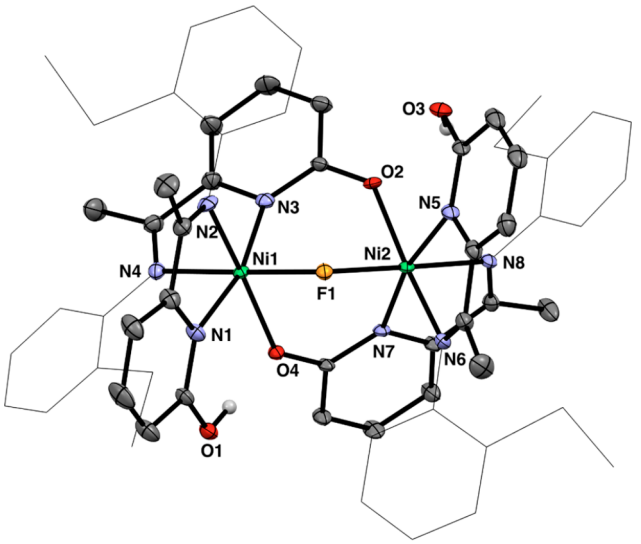

Figure 3. ORTEP diagram for $[(\mu\text{-F})Ni_2(\kappa N,N,O\text{-}\mathbf{1}^-)_2(\kappa N,N\text{-}\mathbf{1})_2](BF_4)$ (**2**) as 30% probability thermal ellipsoids. Aromatic and aliphatic hydrogens, counterion, and the H_2O solvent molecule are omitted for clarity.

symmetric Ni−Ni dimer bridged by two pyridonate ligands and one μ_2-F^- anion. The complex has an overall charge of 1+ and is balanced by a BF_4^- counterion. Interestingly, the thioether sulfur atom was never found to coordinate the nickel center. In the initial structure solution for complex **2**, the bridging ligand was assigned as a μ_2-OH^- anion; however, we were unable to calculate the position of a hydrogen atom associated with the bridging oxygen atom. The ligand could not be a μ_2-O^{2-}, as that would provide an overall neutral charge (not possible due to the BF_4^- counterion in the unit cell). Assigning the bridging atom as O gave R1 = 0.0854 and wR2 = 0.2392 after refinement, whereas the assignment as F provided improved *R* values of R1 = 0.0847 and wR2 = 0.2380.

Cleavage of BF_4^- to form fluoride ions in the presence of transition metals has been reported,[26−33] although it is a rare observation and only occurs only in systems with strong N-heterocyclic ligands such as pyridines, pyrazoles, and imidazoles. The decomposition is thought to be the result of F coordination of BF_4^- to a coordinately unsaturated metal center (ML_n) followed by B−F bond cleavage to yield a $[ML_{n-1}F]^-$ complex and a $L{\cdot}BF_3$ adduct.[27] A more recent report proposes that activation of BF_4^- is facilitated in bimetallic systems wherein μ-F coordination of BF_4^- forms a $M{-}F^{BF3}{-}M$ bridged intermediate. BF_3 then eliminates to form a M−F−M bimetallic complex.[28] Additionally, the relatively long C1−O1 and C29−O3 bond

https://dx.doi.org/10.1021/acs.organomet.9b00799
Organometallics XXXX, XXX, XXX−XXX

lengths of 1.289(8) and 1.292(9) Å, respectively, provide evidence that the nonbridging NNS ligands exist in the pyridonate tautomer rather than the pyridone tautomer. This tautomeric form is stabilized by both coordination to Ni and interaction with the nearby proton.

*[Ni_2(**1**)$_4$(Cl)] (**3**).* The complex [(μ-Cl)Ni_2(κ*N,N,O*-**1**$^-$)$_2$(κ*N,N*-**1**$^-$)(κ*N,N*-**1**)] (**3**) was synthesized in a fashion similar to that for complex **2**: *in situ* deprotonation of **1** using sodium hydride followed by reaction with nickel(II) chloride hydrate. Again, no solvent dependence was observed for this system, and green, blocklike crystals of **3** were always isolated as the sole product. The structure of **3** (Figure 4) is extremely

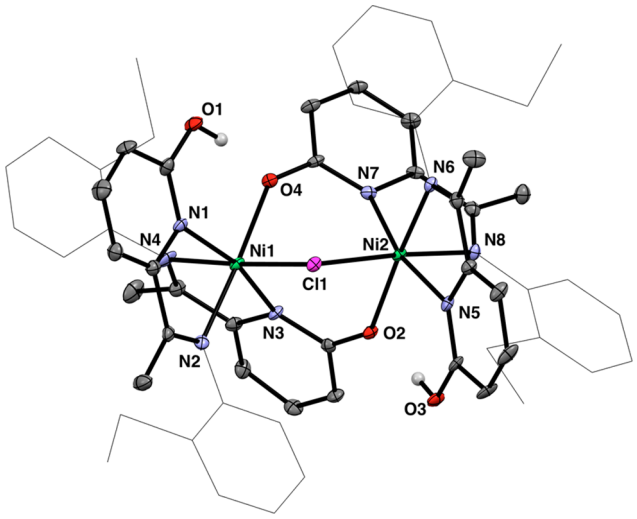

Figure 4. ORTEP diagram for [(μ-Cl)Ni_2(κN,N,O-**1**$^-$)$_2$(κN,N-**1**$^-$)(κN,N-**1**)] (**3**) shown as 30% probability thermal ellipsoids. Aromatic and aliphatic hydrogens, counterion, and Et_2O solvent molecule are omitted for clarity.

similar to that of **2**, differing in only three minor points. (i) Complex **2** contains a bridging μ_2-F$^-$ ligand instead of the μ_2-Cl$^-$ found in **3**. (ii) Complex **2** is a 1+ complex where both nonbridging pyridone ligands are protonated, whereas **3** is a neutral complex where only one nonbridging pyridone is protonated (crystallographically modeled showing both O1 and O3 as protonated, where their respective hydrogen atoms are given occupancy 0.5). (iii) Ignoring the different bridging halides, the bond connectivity in **2** is the mirror image of that in **3**.

*Ni_2(**1**)$_3$(OAc)$_2$(OH_2) (**4**).* For the Ni(OAc)$_2$ system, the metal-bound acetate was used to deprotonate **1** in the presence of Ni(II). Thus, the complex [(μ-OH_2)Ni_2(**1**)$_3$(OAc)$_2$] (**4**) was synthesized by simply adding nickel(II) acetate hydrate to a solution of **1** to give a dark yellow solution. This system did exhibit an effect of solvent on the nuclearity of the isolated product. Reactions and crystallizations carried out in MeCN or DCM resulted in green crystals of **4**. After extensive structure refinement, it was determined that **4** was a co-crystallized mixture of the two structural isomers **4a** and **4b** (Figure 5). In isomer **4a** [(μ-OH_2)Ni_2(κ*N,N,O*-**1**$^-$)(κ*N,N*-**1**$^-$)((κ*N,N*-**1**)(μ-OAc)(OAc)], Ni2 is ligated by one κ*N,N*-**1** ligand, one terminal acetate, and one μ-OAc bridging Ni2 and Ni1. In isomer **4b** [Ni_2(κ*N,N,O*-**1**$^-$)$_2$(κ*N,N*-**1**)(OAc)$_2$(μ-OH_2)], both acetate ligands are terminal and are bound to Ni2 while the two nickel centers are bridged by a κ*N,N,O*-**1**$^-$ pyridone ligand (in addition to the bridging water and bridging κ*N,N,O*-**1**$^-$ pyridone present in both isomers). The aforementioned ligands about Ni2 in isomer **4a** were calculated to have an occupancy of 0.66, while the ligands about Ni2a in isomer **4b** had an occupancy of 0.34. It is interesting that, while different ligands are involved, a bridging motif analogous to that seen in complexes **2** and **3** is present in complexes **4a** and **4b**: namely, two octahedral Ni centers bridged by two anionic 1,3-ligands (pyridonate and/or acetate) and one μ_2 ligand (F$^-$, Cl$^-$, or OH_2).

*Ni(**1**)$_2$($MeOH$)$_2$ (**5**) and Ni(**1**)$_2$(OAc)(OH_2) (**6**).* The mononuclear complexes [Ni(κ*N,N*-**1**$^-$)$_2$($MeOH$)$_2$] (**5**) and [Ni(κ*N,N*-**1**$^-$)(κ*N,N*-**1**)(OAc)(OH_2)] (**6**) are remarkable in that they are the only monomeric Ni complexes characterized in this study, especially considering the propensity of the acetate anion to bridge multiple metal centers. Metalation of **1** was achieved with nickel(II) acetate in MeOH, resulting in a dark yellow-brown solution, and this reaction product was crystallized from MeOH by slow vapor diffusion of diethyl ether to afford yellow blocklike crystals. Complex **5** contains one Ni center ligated by two deprotonated NNS ligands and two solvent methanol ligands (Figure 6). It is interesting to note that, although the oxygen atoms do not ligate the nickel center, the two NNS ligands exist in their pyridonate tautomer, as evidenced by relatively long CO bond lengths of 1.282(3) and 1.284(5) Å

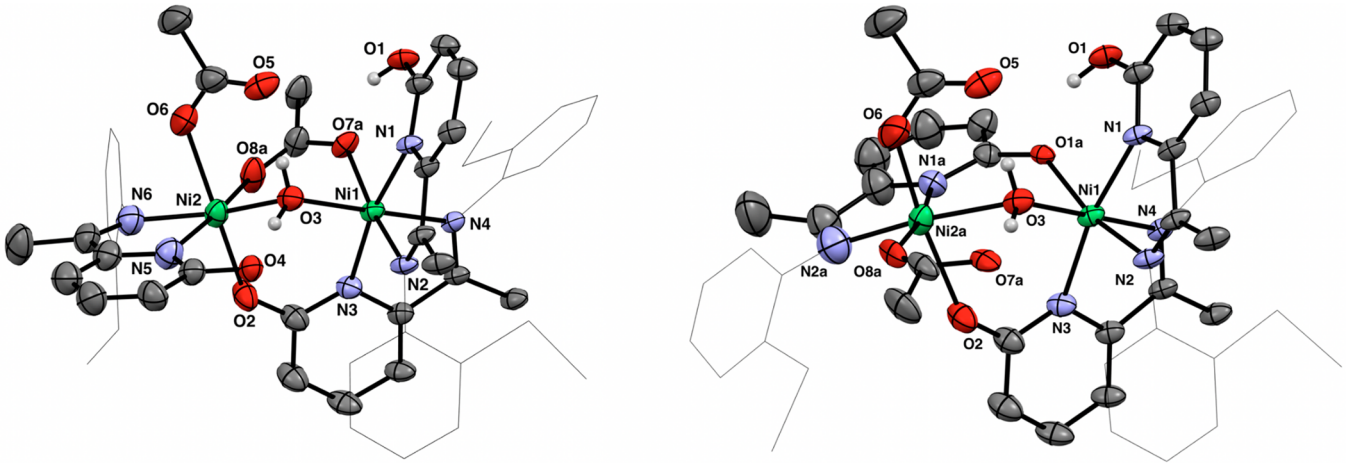

Figure 5. ORTEP diagrams (30% probability thermal ellipsoids) for the coincident structural isomers **4a** (left) and **4b** (right) of general formula [(μ-OH_2)Ni_2(**1**)$_3$(OAc)$_2$] present in the crystal structure of **4**. Aromatic and aliphatic hydrogens are omitted for clarity.

https://dx.doi.org/10.1021/acs.organomet.9b00799
Organometallics XXXX, XXX, XXX−XXX

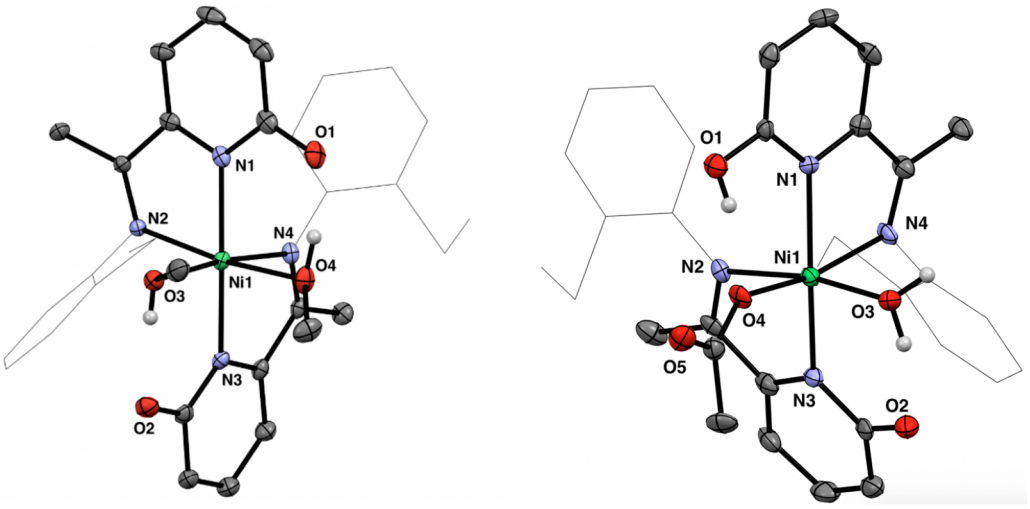

Figure 6. ORTEP diagrams for $[Ni(\kappa N,N\text{-}\mathbf{1}^{-})_2(MeOH)_2]$ (**5**) (left) and $[Ni(\kappa N,N\text{-}\mathbf{1}^{-})(\kappa N,N\text{-}\mathbf{1})(OAc)(OH_2)]$ (**6**) (right) shown as 30% probability thermal ellipsoids. Aromatic and aliphatic hydrogens and solvent molecules are omitted for clarity.

Table 1. Selected Bond Lengths for 1−6 (Å)

	1	2	3	4	5	6
Ni···Ni		Ni1−Ni2 3.382(4)	Ni1−Ni2 3.558(1)	Ni1−Ni2 3.384(3)		
C−O		C1−O1 1.289(7)	C43−O4 1.279(3)	C15−O2 1.28(1)	C15−O2 1.282(3)	C15−O2 1.301(0)
		C29−O3 1.293(9)	C15−O2 1.283(1)	C29−O4 1.29(2)	C1−O1 1.304(5)	C1−O1 1.311(1)
C−OH		C29−O3 1.312(7)	C29−O3 1.314(6)	C1−O1 1.335(6)		
		C1−O1 1.315(3)	C1−O1 1.331(1)			
C═O	C1−O1 1.246(5)					
$Ni-N^{py}$		Ni2−N7 2.085(5)	Ni1−N3 2.081(3)	Ni2−N5 2.02(1)	Ni1−N3 2.087(3)	Ni1−N3 2.070(8)
		Ni1−N3 2.095(2)	Ni1−N1 2.082(3)	Ni1−N3 2.071(5)	Ni1−N1 2.088(0)	Ni1−N1 2.125(8)
		Ni1−N1 2.123(7)	Ni2−N7 2.093(7)	Ni1−N1 2.104(5)		
		Ni2−N5 2.123(7)	Ni2−N5 2.094(8)			
$Ni-N^{imine}$		Ni2−N8 2.075(1)	Ni1−N4 2.088(4)	Ni2−N6 2.055(8)	Ni1−N2 2.091(2)	Ni1−N2 2.089(8)
		Ni1−N2 2.091(7)	Ni2−N8 2.089(0)	Ni1−N4 2.085(5)	Ni1−N4 2.104(4)	Ni1−N4 2.092(8)
		Ni1−N4 2.092(9)	Ni2−N6 2.092(2)	Ni1−N2 2.112(3)		
		Ni2−N6 2.104(9)	Ni1−N2 2.094(7)			

(Table 1 for selected bond lengths for compounds **1**−**6**). Complex **6** was serendipitously isolated and characterized in an attempt to obtain higher quality crystals of **4**. After **1** was reacted with nickel acetate in MeCN, the yellow solution was evaporated at −20 °C, and dark yellow crystals suitable for diffraction were obtained. Surprisingly, $[Ni(\kappa N,N\text{-}\mathbf{1}^{-})(\kappa N,N\text{-}\mathbf{1})(OAc)(OH_2)]$ (**6**) was found to be the resulting structure (Figure 6). Complex **6** is a nickel monomer with a structure similar to that of **5**; however, **6** contains an acetate and a water ligand instead of two methanol ligands. Complex **6** contains one protonated pyridinol ligand and one deprotonated pyridonate ligand, thus maintaining a neutral overall charge for the complex.

UV/Vis Spectroscopy: Solution versus Solid State. The results of the complexation of **1** with nickel(II) acetate presented an interesting conundrum. Crystals of **4** (note that **4** is a 2:1 mixture of isomers as detailed earlier) and **6** were obtained from the same solution: 1 equiv of nickel(II) acetate and 1 equiv of **1** dissolved in MeCN; however, different crystallization methods yielded different solid-state structures, as determined by XRD. As detailed in the preceding sections, slow vapor diffusion of Et_2O into MeCN yielded crystals of **4**, while slow evaporation of the MeCN solution yielded crystals of **6**. It is logical to conclude that since the same reaction can yield both **4** and **6**, it is the crystallization process that determines which of these complexes is isolated in the solid state. It must be the case that (i) both **4** and **6** exist in solution, perhaps interconverting until preferential crystallization drives one to crystallize, or (ii) some other Ni−pyridone complex exists in solution, which then converts to **4** or **6** depending on the method of crystallization. To spectroscopically probe the difference in solid- and solution-state structures of **4** and **6**, UV/vis spectroscopy was utilized. The absorption spectra of **4** and **6** in both the solid and solution states is shown in Figure 7. To obtain UV/vis spectra of **4** and **6** in the solid state, the diffuse reflectance spectra of each were acquired, and the data were converted to pseudoabsorbance using the Kubelka−Munk model.[36] Complexes **4** and **6** have distinct diffuse reflectance solid-state spectra, showing three main absorbances corresponding to two spin-allowed transitions of an octahedral d^8 system: $^3A_{2g} \rightarrow {}^3T_{1g}$ and $^3A_{2g} \rightarrow {}^3T_{2g}$. Additionally, one spin-forbidden transition is observed at approximately 790 nm corresponding to a $^3A_{2g} \rightarrow {}^1E_g$ transition. This is consistent with the already established single-crystal structures of **4** and **6**, which contained octahedral Ni(II). In contrast, samples of **4** and **6** dissoved in DCM exhibit identical absorbance spectra, neither of which bear any resemblance to the diffuse reflectance spectra of **4** and **6**. Specifically, solutions

https://dx.doi.org/10.1021/acs.organomet.9b00799
Organometallics XXXX, XXX, XXX−XXX

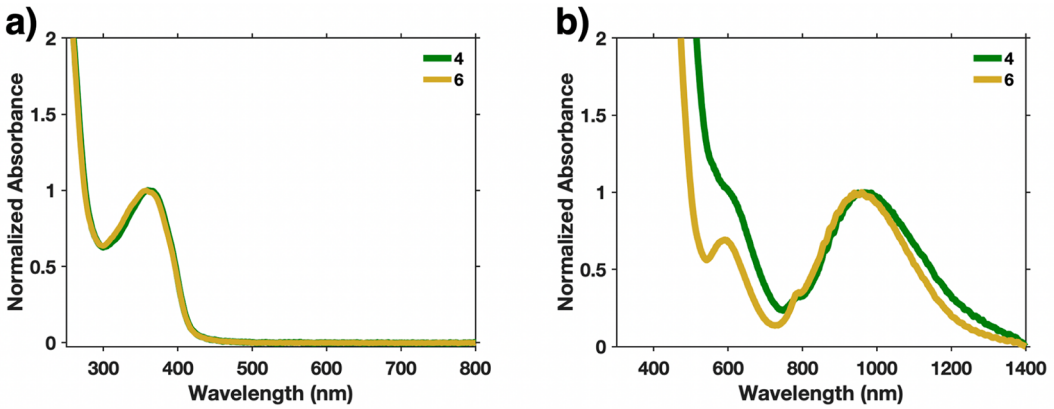

Figure 7. UV/vis spectra: (a) absorbance spectra of dimeric **4** and monomeric **6** in DCM solution (**4**, λ = 360 nm; **6**, λ = 360 nm); (b) diffuse reflectance (converted to absorbance) spectra of **4** and **6** (powderized crystals) (**4**, λ = 589, 793, 958 nm; **6**, λ = 591, 789, 987 nm).

Scheme 3. Proposed Square-Planar Structure of the Solution Species 7 and Its Conversion to 4 and 6[a]

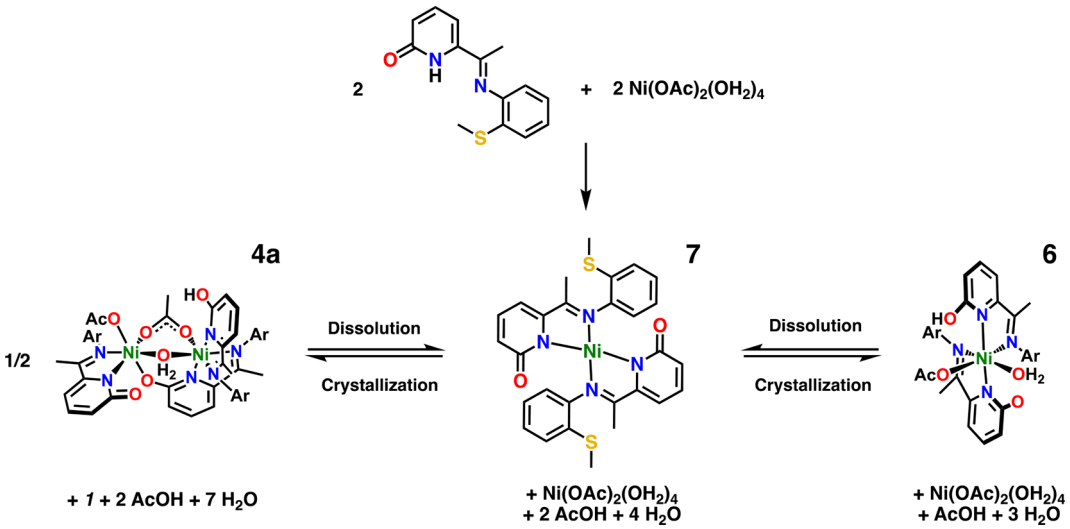

[a]Only isomer **4a** is shown for the sake of simplicity. Note that the stoichiometry described here is accurate only in a closed system, wherein the solid products **4** or **6** are not isolated. If they are isolated, **4** and **6** will redissolve to regenerate **7**; however, the stoichiometry will be different.

of **4** and **6** exhibit one strong absorbance at 360 nm (ε = 5640 M^{-1} cm^{-1}), which is indicative of a square-planar d^8 metal complex. The absence of any features in the near-IR region (800−1200 nm) corroborates the assignment of this solution-state species as a square-planar Ni(II) complex, as octahedral and tetrahedral complexes will exhibit weak, Laporte-forbidden d−d transitions in the NIR ($^3A_{2g} \rightarrow {}^3T_{2g}$ for octahedral and $^2B_{1g} \rightarrow {}^2B_{2g}$ for tetrahedral). A single peak in the range of 300−500 nm is characteristic of square-planar Ni(II) complexes and is typically ascribed to either a d−d transition between the nearly degenerate $e_g(d_{xz},d_{yz})$, $b_{2g}(d_{xy})$, and $a_{1g}(d_{z^2})$ nonbonding manifold and either an antibonding $b_{1g}(d_{x^2-y^2})$ level (weak field case) or a ligand to metal charge transfer (MLCT) from a ligand σ-bonding orbital to said nonbonding manifold. The fairly high extinction coefficient for this feature indicates that the transition is primarily MLCT in nature.[34]

We thus propose that the solution structure of **4** and **6** is a square-planar complex. As the complex is soluble in nonpolar solvents such as DCM, it is likely neutral. Since DCM is nominally noncoordinating, it is also unlikely that the complex contains a solvato ligand (MeCN if dissolved in acetonitrile, MeOH or MeO^- if dissolved in methanol, etc.). Finally, it is unlikely that **1** coordinates Ni(II) in a κNNS pincer fashion, as in all previous structures characterized in this study the coordination of the thioether sulfur is outcompeted by weaker ligands such as water and methanol. High-resolution mass spectrometry (ESI+) showed an $[M + H]^+$ parent ion peak at m/z = 573.0926, corresponding to a molecular formula of $[C_{28}H_{27}N_4NiO_2S_2]^+$ (calculated m/z = 573.09230). This evidence supports the solution-state species as $[Ni(\kappa N,N\text{-}\mathbf{1}^-)_2]$ (**7**), whose structure is depicted in Scheme 3. Considering that ligand **1** and $Ni(OAc)_2(OH_2)_4$ were reacted in a 1:1 molar ratio, it is reasonable that, after complexation to generate **7**, excess acetate, water, and nickel(II) remain in solution. These species then react with **7** under the conditions of crystallization to form **4** or **6**.

Spectroscopic characterization of the discrepancy between the solid- and solution-state structures of nickel−pyridone complexes provides some insight into the curious observation made by Winpenny and co-workers in their work synthesizing polynuclear nickel pyridone clusters. These researchers reported that different crystal structures were obtained when the product of a given reaction was crystallized using different solvents and specifically that polar protic solvents such as methanol and

https://dx.doi.org/10.1021/acs.organomet.9b00799
Organometallics XXXX, XXX, XXX−XXX

ethanol yield clusters of lower nuclearity while polar aprotic solvents such as THF and DCM yield clusters of high nuclearity. For example, nickel acetate was reacted with 6-chloro-2-pyridone, affording a linear trinuclear nickel cluster on crystallization from MeOH/Et_2O. Crystallization of the same reaction product from THF/Et_2O resulted in a cyclic dodecanuclear nickel cluster.[35] We hypothesize that the same phenomenon observed in our system is responsible for the variety of crystalline products obtained from a single set of reaction conditions by Winpenny and co-workers: namely, the existence of some distinct solution-state species whose solid-state structure is highly dependent upon the crystallization method.

Magnetic Susceptibility. For many multimetallic Ni–pyridone clusters, extensive ferromagnetic or antiferromagnetic coupling between metal centers has been reported.[15−17,35] To probe this effect for the three bimetallic complexes **2**–**4**, room-temperature benchtop magnetic susceptibility measurements were obtained. The monometallic complexes **5** and **6** exhibited effective magnetic moments of 2.88 and 2.89 μ_B, respectively—expected values for an S = 1 octahedral Ni(II) complex. However, complexes **2**–**4** were found to have effective magnetic moments of less than 5.66 μ_B (Table 2)—the expected additive spin-only value for a complex with two uncoupled octahedral Ni(II) centers. Such low magnetic moments indicate weak antiferromagnetic coupling occurring between the two Ni centers of complexes **2**–**4**.

Table 2. Room Temperature Magnetic Moments for Complexes 2−6

complex	χ_m (10^{-3} cm mol^{-1})	μ_{eff} (μ_B)
2	7.26	4.12
3	7.67	4.24
4	7.00	4.05
5	3.55	2.88
6	3.57	2.89

CONCLUSION

The main findings of this work are summarized as follows.

(1) The NNS ligand **1** provides a wide range of coordinating motifs in mononuclear and dinuclear Ni(II) complexes. However, the Schiff base N and pyridone N donors always coordinate the metal center, while the thioether S does not bind Ni(II) in any solid-state structures.

(2) The pyridone *ortho* position (O atom) is the driver of coordination motif diversity. Depending on the metal-bound state (free ligand, O unbound, monodentate, or μ_2-bridging), this functional group provides coordination modes and C···O bond distances that are consistent with its formulation as pyridone ($_{py}C{=}O$), pyridinol ($_{py}C{-}OH$), pyridinolate ($_{py}C{-}O^-$) and intermediate resonant structure ($_{py}C^{1.5}{-}O^{\delta-}$).

(3) The presence of crystal structures with both (a) nickel-bound acetate moieties (monodentate and bidentate-bridging) coincident with (*b*) nickel-bound pyridone, pyridinol, and pyridonate motifs suggests that the pK_a values for acetate (pK_a = 4.75) and the metal-bound pyridinol are very similar (for reference, pK_{a1} for metal-bound 6,6′-dihydroxybipyridine derivatives ranges between 4.5 and 5.6).[39,40]

(4) Much evidence supports the claim that pyridone ligands (such as that used in this study) provide an extremely soft conformational coordination landscape for divalent metal ions. The primary evidence is as follows.

  (a) The minor change from fluoride-bridged **1** (BF_4^- counterion) to chloride-bridged **2** (neutral species) also involves a change in pyridone(s) protonation state in **1** (two free $_{py}C{-}OH$ units) versus **2** (two free $_{py}C{\cdots}O^{\delta-}$ units share one proton; i.e. two half-occupancy H atoms)

  (b) Upon metalation with nickel(II) acetate, three different X-ray structures (**4**–**6**) can be observed depending on the method of crystallization.

  (c) Coincident isomers are found in the X-ray structure of **4**: namely, **4a** (one μ_2-bridging pyridonolate-O atom; one bridging acetate) and **4b** (two μ_2-bridging pyridonate-O atoms; no bridging acetates).

  (d) There is a clear discrepancy between all of the solid-state X-ray structures and the solution-state structures as determined by UV/vis spectroscopy (vide infra).

(5) Finally, UV/vis spectroscopy on both the isolated solids (reflectance) and solutions (absorbance) reveal that the *none* of the solid-state structures exist in solution. The absence of any low-energy d−d transitions—as expected for octahedral Ni(II)—suggest that all solutions contain square-planar Ni(II) species with the proposed structure [Ni(κN,N-$\mathbf{1}^-$)$_2$], as additionally evidenced by high-resolution mass spectrometry.

(6) All solid-state complexes contain high-spin (S = 1) nickel(II) centers, and the dinuclear complexes exhibit some extent of magnetic coupling, as evidenced by μ_{eff} values that are significantly lower than the expected spin-only values.

All of the above observations are cause for a re-examination of the structural dynamics of transition-metal–pyridone systems. While this work has little effect on the existing literature which examines the solid-state properties of transition-metal–pyridone complexes, the discrepancy in the solid-state and solution-state structures of these molecules may prove an important consideration in the applications of pyridone ligands in transition-metal reactivity and catalysis. Transition-metal–pyridone complexes characterized crystallographically as polynuclear clusters, presumed to be for all intents and purposes substitutionally inert, may prove to adopt a different structure in solution, perhaps one more desirable for reactivity.

ASSOCIATED CONTENT

Supporting Information

The Supporting Information is available free of charge at https://pubs.acs.org/doi/10.1021/acs.organomet.9b00799.

Crystallographic information for compounds **1**–**6** (PDF)

Accession Codes

CCDC 1967314–1967315, 1967320–1967321, 1967326, and 1967334 contain the supplementary crystallographic data for this paper. These data can be obtained free of charge via www.ccdc.cam.ac.uk/data_request/cif, or by emailing data_request@ccdc.cam.ac.uk, or by contacting The Cambridge Crystallographic Data Centre, 12 Union Road, Cambridge CB2 1EZ, UK; fax: +44 1223 336033.

https://dx.doi.org/10.1021/acs.organomet.9b00799
Organometallics XXXX, XXX, XXX−XXX

AUTHOR INFORMATION

Corresponding Author

Michael J. Rose − *Department of Chemistry, The University of Texas at Austin, Austin, Texas 78712, United States;* orcid.org/0000-0002-6960-6639; Email: mrose@cm.utexas.edu

Authors

Sean T. Goralski − *Department of Chemistry, The University of Texas at Austin, Austin, Texas 78712, United States;* orcid.org/0000-0002-4169-338X

Taylor A. Manes − *Department of Chemistry, The University of Texas at Austin, Austin, Texas 78712, United States*

Simone E. A. Lumsden − *Department of Chemistry, The University of Texas at Austin, Austin, Texas 78712, United States*

Vincent M. Lynch − *Department of Chemistry, The University of Texas at Austin, Austin, Texas 78712, United States*

Complete contact information is available at: https://pubs.acs.org/10.1021/acs.organomet.9b00799

Notes

The authors declare no competing financial interest.

ACKNOWLEDGMENTS

This work was supported by the National Science Foundation (CHE-1808311) and the Welch Foundation (F-1822). The authors express their gratitude to Jon Bender for his assistance in obtaining and interpreting UV/vis spectra, as well as Prof. Sean Roberts for providing access to the UV/vis spectrophotometer.

REFERENCES

(1) Cotton, F. A.; Fanwick, P. E.; Niswander, R. H.; Sekutowski, J. C. A triad of homologous air-stable compounds containing short, quadruple bonds between metal atoms of Group 6. *J. Am. Chem. Soc.* **1978**, *100*, 4725−4732.

(2) Cotton, F. A.; Thompson, J. L. A triple bond between osmium atoms. Preparation and structure of dichlorotetrakis(2-hydroxypyridinato)diosmium(III). *J. Am. Chem. Soc.* **1980**, *102*, 6437−6441.

(3) Cotton, F. A.; Ilsley, W. H.; Kaim, W. Homologous chromium, molybdenum, and tungsten derivatives of 6-chloro-2-hydroxypyridine. Inductive effects on the metal-metal bond length. *Inorg. Chem.* **1980**, *19* (6), 1453−1457.

(4) Blake, A.; Grant, C.; Parsons, S.; Rawson, J.; Winpenny, R. The synthesis, structure and magnetic properties of a cyclic dodecanuclear nickel complex. *J. Chem. Soc., Chem. Commun.* **1994**, 2363−2364.

(5) Kakaroni, F.; Collet, A.; Sakellari, E.; Tzimopoulos, D.; Siczek, M.; Lis, T.; Murrie, M.; Milios, C. Constructing Cr^{III}-centered heterometallic complexes: $[Ni^{II}_6Cr^{III}]$ and $[Co^{II}_6Cr^{III}]$ wheels. *Dalton Trans.* **2018**, *47*, 58−61.

(6) Kelson, E. P.; Phengsy, P. P. Synthesis and structure of a ruthenium(II) complex incorporating *N*-bound 2-pyridonato ligands; a new catalytic system for transfer hydrogenation of ketones. *Dalton Trans.* **2000**, *22*, 4023−4024.

(7) Moore, C.; Szymczak, N. 6,6′-Dihydroxy terpyridine: a proton-responsive bifunctional ligand and its application in catalytic transfer hydrogenation of ketones. *Chem. Commun.* **2013**, *49*, 400−402.

(8) Paul, B.; Chackrabarti, K.; Kundu, S. Optimum difunctionality in a 2-(2-pyridyl-2-ol)-1,10-phenanthroline based ruthenium complex for transfer hydrogenation of ketones and nitriles: impact of the number of 2-hydroxypyridine fragments. *Dalton Trans.* **2016**, *45*, 11162−11171.

(9) Shi, J.; Hu, B.; Gong, D.; Shang, S.; Hou, G.; Chen, D. Ruthenium complexes bearing an unsymmetrical pincer ligand with a 2-hydroxypyridylmethylene fragment: active catalysts for transfer hydrogenation of ketones. *Dalton Trans.* **2016**, *45*, 4828−4834.

(10) Yamaguchi, R.; Kobayashi, D.; Shimizu, M.; Fujita, K. Synthesis of a series of iridium complexes bearing substituted 2-pyridonates and their catalytic performance for acceptorless dehydrogenation of alcohols under neutral conditions. *J. Organomet. Chem.* **2017**, *843*, 14−17.

(11) Toyomura, K.; Fujita, K. Synthesis of coorinatively unsaturated iridium complexes having functional 8-quinolinolato ligands: new catalysts for dehydrogenative oxidation of alcohols in aqueous media. *Chem. Lett.* **2017**, *46*, 808−810.

(12) Gerlach, D. L.; Bhagan, S.; Cruce, A. A.; Burks, D. B.; Nieto, I.; Truong, H. T.; Kelley, S. P.; Herbst-Gervasoni, C. J.; Jernigan, K. L.; Bowman, M. K.; Pan, S.; Zeller, M.; Papish, E. T. Studies of the pathways open to copper water oxidation catalysts containing proximal hydroxyl groups during electrocatalysis. *Inorg. Chem.* **2014**, *53*, 12689−12698.

(13) DePasquale, J.; Nieto, I.; Reuther, L.; Herbs-Gervasoni, C.; Paul, J.; Mochalin, V.; Zeller, M.; Thomas, C.; Addison, A.; Papish, E. Iridium dihydroxybipyridine complexes show that ligand deprotonation dramatically speeds rate of catalytic water oxidation. *Inorg. Chem.* **2013**, *52*, 9175−9183.

(14) Mao, Q.; Pang, Y.; Li, X.; Chen, G.; Tan, H. Theoretical study of the mechanisms of two copper water oxidation electrocatalysts with bipyridine ligands. *ACS Catal.* **2019**, *9*, 8798−8809.

(15) Brechin, E.; Clegg, W.; Murrie, M.; Parsons, S.; Teat, S.; Winpenny, R. Nanoscale cages of manganese and nickel with "rock salt" cores. *J. Am. Chem. Soc.* **1998**, *120*, 7365−7366.

(16) Langley, S.; Helliwell, M.; Teat, S.; Winpenny, R. Synthesis and characterization of nickel(II) phosphonate complexes utilizing pyridonates and carboxylates as co-ligands. *Inorg. Chem.* **2014**, *53* (2), 1128−1134.

(17) Benelli, C.; Blake, A.; Brechin, E.; Coles, S.; Graham, A.; Harris, S.; Meier, S.; Parkin, A.; Parsons, S.; Seddon, A.; Winpenny, R. A family of polynuclear cobalt and nickel complexes stabilized by 2-pyridonate and carboxylate ligands. *Chem. - Eur. J.* **2000**, *6* (5), 883−896.

(18) Graham, A.; Meier, S.; Parsons, S.; Winpenny, R. Changing cage structures through inter-ligand repulsions. *Chem. Commun.* **2000**, 811−812.

(19) Chakraborty, S.; Piszel, P. E.; Brennessel, W. W.; Jones, W. D. A single nickel catalyst for the acceptorless dehydrogenation of alcohols and hydrogenation of carbonyl compounds. *Organometallics* **2015**, *34*, 5203−5206.

(20) Santana, M. D.; Garcia, G.; Rufete, A.; Sanchez, G.; de Arellano, M. C. R.; Lopez, G. Preparation, NOSEY characterisation and structure of $[Ni(N_3\text{-macrocycle})(hp)]ClO_4$: the first crystallographic characterised mononuclear nickel complex containing the 2-pyridonate (hp) ligand. *Inorg. Chem. Commun.* **1998**, *1*, 267−269.

(21) Pan, N.; Wie, R.; Chi, Y.; Shi, J.; Wie, W.; Zhang, Y. Intermolecular interaction and magnetic coupling mechanism of a mononuclear nickel(II) complex. *Z. Anorg. Allg. Chem.* **2013**, *639*, 1026−1031.

(22) Liu, Q.; Liu, Q.; Zhao, Q. Diaqua(1,10-phenanthrolin-2-ol)nickel(II) dinitrate. *Acta Crystallogr., Sect. E: Struct. Rep. Online* **2009**, *65*, No. m883.

(23) Kukovec, B.; Vaz, P.; Calhorda, M.; Popovic, Z. Disappearing and concomitant polymorphism of nickel(II) complexes with 6-hydroxypicolinic acid. Structural and density functional theory studies. *Cryst. Growth Des.* **2010**, *10*, 3685−3693.

(24) Parsons, S.; Winpenny, R. Structural chemistry of pyridonate complexes of late 3d-metals. *Acc. Chem. Res.* **1997**, *30*, 89−95.

(25) Peng, D.; Zhang, Y.; Du, X.; Zhang, L.; Leng, X.; Walter, M.; Huang, Z. Phosphinite-iminopyridine iron catalystst for chemoselective alkene hydrosilylation. *J. Am. Chem. Soc.* **2013**, *135* (51), 19154−19166.

(26) Muthiah, K.; Durgaprasad, G.; Xie, Z.; Williams, O.; Joseph, C.; Lynch, V.; Rose, M. Mononuclear iron(II) dicarbonyls derived fromn NNS ligands − structural models related to a "pre-acyl" active site of mono-iron (Hmd) hydrogenase. *Eur. J. Inorg. Chem.* **2015**, *2015*, 1675−1691.

https://dx.doi.org/10.1021/acs.organomet.9b00799
Organometallics XXXX, XXX, XXX−XXX

(27) Reedijk, J. Formation of fluoride-containing coordination compounds by decomposition of transition metal tetrafluoroborates. *Comments Inorg. Chem.* **1982**, *1*, 379−389.
(28) Das, R.; Ghatak, T.; Samanta, R.; Bera, J. A fluoro-bridged dinuclear nickel(II) compound from tetrafluoroborate precursor: making sense of a serendipitous reaction. *Indian J. Chem.* **2011**, *50A*, 1350−1355.
(29) Xiang, W.; Luo, Q.; Jiang, H.; Meng, X.; Li, R.; Zhang, J.; Peng, T. New Ni(II) complexes based on N'NN' pincer ligands: syntheses, structures and B−F cleavage of BF_4−promoted by a di-cationic Ni(II) center. *J. Coord. Chem.* **2016**, *69* (15), 2353−2363.
(30) Zimmermann, T. P.; Dammers, S.; Stammler, A.; Bogge, H.; Glaser, T. Reactivity differences for the oxidation of $Fe^{II}Fe^{III}$ to $Fe^{III}(\mu$-$O)Fe^{III}$ complexes caused by pyridyl versus 6-methyl-pyridyl ligands. *Eur. J. Inorg. Chem.* **2018**, *2018*, 5229−5237.
(31) Augenstein, T.; Dorner, F.; Reiter, K.; Wagner, H.; Garnier, D.; Klopper, W.; Breher, F. A boron-fluorinated tris(pyrazolyl)borate ligand (^{F}Tp*) and its mono- and dinuclear copper complexes $[Cu(^{F}Tp^*)_2]$ and $[Cu_2(^{F}Tp^*)_2]$: synthesis, structures, and DFT calculations. *Chem. - Eur. J.* **2016**, *22*, 7935−7943.
(32) Huxel, T.; Leone, S.; Lan, Y.; Demeshko, S.; Klingele, J. 2-amino-4-(2-pyridyl)thiazole as chelating ligand: a dinuclear oxido-bridged ferric complex and mononuclear 3d metal complexes. *Eur. J. Inorg. Chem.* **2014**, *2014*, 3114−3124.
(33) Cho, Y.; Ward, M.; Rose, M. Substituent effects of N4 Schiff base ligands on the formation of fluoride-bridged dicobalt(II) complexes via B−F abstraction: structures and magnetism. *Dalton Trans.* **2016**, *45*, 13466−13476.
(34) Lever, A. *Inorganic Electronic Spectroscopy*; Elsevier: 1968; pp 343−344.
(35) Breeze, B.; Shanmugam, M.; Tuna, F.; Winpenny, R. A series of nickel phosphonate-carboxylate cages. *Chem. Commun.* **2007**, *48*, 5185−5187.
(36) Kubelka, P.; Munk, F. Ein Beitrag zur Optik der Farbenstriche. *Zeits für Techn. Phys.* **1931**, *12*, 593−601.
(37) Gerlach, D.; Nieto, I.; Herbst-Gervasoni, C.; Ferrence, G.; Zeller, M.; Papish, E. Crystal structure of bis- and hexakis[6,6'-dihydroxybipyridine)copper(II)] nitrate coordination complexes. *Acta Crystallogr.* **2015**, *E71*, 1447−1453.
(38) Fujita, K.; Tanino, N.; Yamaguchi, R. Ligand-promoted dehydrogenation of alcohols catalyzed by Cp*Ir Complexes. A new catalytic system for oxidant-free oxidation of alcohols. *Org. Lett.* **2007**, *9*, 109.
(39) Qu, F.; Park, S.; Martinez, K.; Gray, J.; Thowfike, S.; Lundeen, J.; Kuhn, A.; Charboneau, D.; Gerlach, D.; Lockart, M.; Law, J.; Jernigan, K.; Chambers, N.; Zeller, M.; Piro, N.; Kassel, W.; Schmehl, R.; Paul, J.; Merino, E.; Kim, Y.; Papish, M. Ruthenium complexes are pH-activated metallo prodrugs (pHAMPSs) with light-triggered selective toxicity towards cancer cells. *Inorg. Chem.* **2017**, *56*, 7519−7532.
(40) Burks, D.; Vasiliu, M.; Dixon, D.; Papish, E. Thermodynamic acidity studies of 6,6'-dihydroxy-2,2'-bipyridine: a combined experimental and computational approach. *J. Phys. Chem. A* **2018**, *122*, 2221−2231.

https://dx.doi.org/10.1021/acs.organomet.9b00799
Organometallics XXXX, XXX, XXX−XXX